KSCE Journal of Civil Engineering (0000) 00(0):1-9
DOI 10.1007/s12205-017-1184-7

Geotechnical Engineering
pISSN 1226-7988, eISSN 1976-3808
www.springer.com/12205

Seismic Response of Circular Tunnels in Jointed Rock

Jin-Kwon Yoo*, Jeong-Seon Park, Duhee Park***, and Seung-Won Lee******

Received August 24, 2016/Revised March 21, 2017/Accepted April 28, 2017/Published Online July 10, 2017

Abstract

Although deformation along a weak joint under a strong seismic event can seriously damage the tunnel, the effect of joint has not yet been well understood or quantified. We perform a series of pseudo-static discrete element analyses to evaluate the effect of deformation along rock joint on the seismic response of circular tunnels. We also perform parallel continuum analyses to compare and quantify their differences. A comprehensive set of joint parameters are considered in this study. The results illustrate that the joint significantly increases the moment demand in the tunnel lining, whereas it has a secondary influence on the thrust. The joint stiffness and shear strength have critical influence on the tunnel response. Widely spaced joint set produces a larger tunnel response. The tunnel response is highest for vertical and horizontal joints, and the lowest when the joint dips at an angle of 45°. The moment in jointed rock may be 20 times higher than that in intact rock. The pronounced deviation from continuum analyses highlights the need to estimate the influence of discontinuities on the seismic response of underground tunnels from discrete element analyses. This may be of concern for critical structures such as nuclear facilities.

Keywords: *rock joint, tunnel, seismic response, pseudo-static, discrete element analysis*

1. Introduction

Underground space has been reported to be more resistant to seismically induced damage compared with above-ground structures. However, recent earthquakes have illustrated that even underground structures are susceptible to damage under strong seismic excitations (Asakura and Sato, 1996; Hashash, 2002; Wang, 1993). Considering the importance of underground facilities in urban societies, underground spaces should be designed to withstand strong earthquakes.

Because underground tunnels are surrounded by ground, they are not allowed to freely vibrate and primarily conform to the movement of ground. Analytical pseudo-static solutions have been presented to estimate the tunnel response subjected to shear deformation (e.g. Wang, 1993; Penzien and Wu, 1998). The solutions assume that the tunnel is surrounded by elastic, massless, and continuous medium. The procedure assumes that the response of tunnel lining under dynamic motion can be decoupled from that produced under static condition.

For a realistic simulation, the static stress imposed on the tunnel due to overburden and the tunneling process has to be modeled (Hashash *et al*., 2010). However, extensive comparisons showed that the increment of moment and forces due to seismically induced deformation for the massless condition with zero gravity and for the case where the in-situ static stresses are applied are nearly identical (Ahn, 2013). Numerical pseudo-static analyses, where the tunnel is assumed to be surrounded by massless ground, have been widely performed (Hashash and Park, 2001; Hashash *et al.*, 2003). Dynamic analyses were also performed to simulate the dynamic soil-structure interaction (Asakura and Sato, 1996; Sedarat *et al.*, 2009; Cilingir and Gopal Madabhushi, 2011). Hashash *et al.* (2010) reported that for single box tunnels, the results of pseudo-static and dynamic analyses are almost identical. Argyroudis and Pitilakis (2012) also reported that the difference between the pseudo-static and dynamic analyses is not significant.

Effect of jointed rock on tunneling has been a topic of interest (Barton, 1995). Researchers used the discrete element method to investigate how the joints influence the tunnel (Bhasin and Høeg, 1998; Hao and Azzam, 2005; Vardakos *et al*., 2007). Studies on the influence of jointed rock mass on blast induced vibration propagation have been performed. Hao *et al.* (2001) used the measured motions under in-situ blasting to identify the effect of the joint layout on propagation of stress waves. Li and Ma (2010) studied the interaction between the blast wave and arbitrarily positioned rock joint. Ma and Brady (1999) investigated the performance of an underground excavation in jointed rock under repeated loading.

*Member, Graduate Student, Dept. of Civil and Environmental Engineering, Hanyang University, Seoul 04763, Korea (E-mail: eternal21c@hanyang.ac.kr)
**Post-Doc., Dept. of Civil and Environmental Engineering, Hanyang University, Seoul 04763, Korea (E-mail: jpark86@hanyang.ac.kr)
***Member, Associate Professor, Dept. of Civil and Environmental Engineering, Hanyang University, Seoul 04763, Korea (Corresponding Author, E-mail: dpark@hanyang.ac.kr)
****Senior Geotechnical, Senior Engineer, ARUP, New York, NY 10005, USA (E-mail: sean.Lee@arup.com)

Limited study has been performed to investigate the effect of rock joints on seismic response of tunnels, possibly because the shear deformation in jointed rock is small compared with soil profiles and typically does not lead to structural failure. However, although a tunnel collapse is unlikely to occur in jointed rock, it should be investigated whether localized concentration of the force or moment at the joint-tunnel intersection may cause cracks to develop. The cracks may influence the long-term sustainability of the underground infrastructure. Another concern is the response of nuclear facilities that are built underground, for which even small-scale cracks are not allowed.

In this study, a series of discrete element analyses (DE) were performed to evaluate the influence of rock joints on the seismic response of tunnels. A comprehensive set of joint parameters, which include tunnel-joint intersection location, joint spacing, joint dip, and mechanical properties, were used in the simulation. We also perform parallel continuum analyses to compare with DE and to quantify the difference.

2. Numerical Simulation

UDEC^{2D} (Itasca Consulting Group, 2004) and FLAC^{2D} (Itasca Consulting Group, 2002) were used to perform the DE and continuum analysis, respectively. In UDEC^{2D} (Itasca Consulting Group, 2004), which is the most widely used DE program in the field of geotechnical engineering, the discontinuous medium is represented as an assemblage of discrete blocks and the discontinuities are treated as boundary conditions between the blocks. Large displacements along discontinuities and rotations of blocks are allowed in the program. FLAC^{2D} (Itasca Consulting Group, 2002) uses the finite difference analysis (FD) algorithm to solve boundary value problems.

Figure 1 illustrates the computational domain and the boundary conditions applied in this study. The 2D computational model domain is 50 m by 50 m in height and width, respectively. The lower boundary was fixed in the vertical and horizontal directions, whereas the lateral boundaries were fixed in the vertical direction. The tunnel was modeled as a circular opening at the center of the domain with a radius of 5 m. A 0.3 m thick liner was inscribed around the circumference of the tunnel. Plane strain condition was used in all analyses. As shown in Fig. 2, the

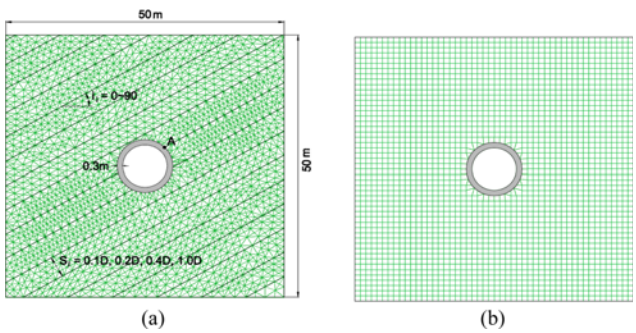

Fig. 1. Computational Model: (a) Discrete Element Analysis Model and Joint Layout, (b) Finite Difference Analysis Model

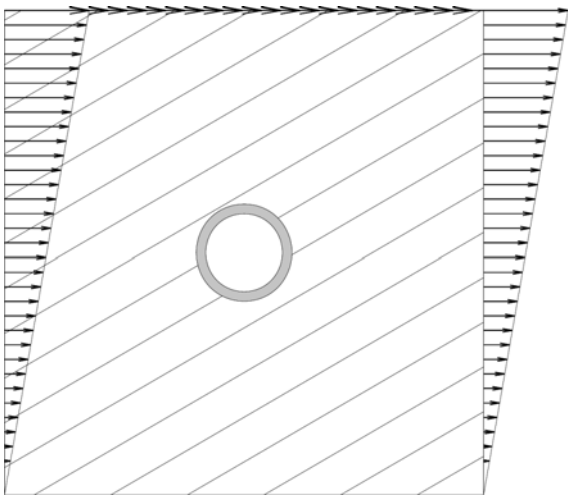

Fig. 2. Application of Displacement Boundary

deformation was imposed as an inverted triangle along the lateral boundaries with a constant displacement at the top boundary.

We did not perform dynamic analyses, because it was reported that the seismic response of underground structures is sufficiently accurately estimated for engineering purposes by the pseudo-static analysis (Hashash *et al.*, 2010; Argyroudis and Pitilakis, 2012). Also based on observations made in previous studies (e.g. Ahn, 2013), we did not apply gravitational load on the tunnel. The calculated response represents the increment of moment and forced induced by ovaling deformation of the tunnel.

In both DE and FD, a mixed discretization scheme is used for the quadrilateral elements, where each quadrilateral zone (element) is subdivided internally into two overlaid constant-strain-triangles (CST). It was reported that the scheme can accurately model the plastic collapse load (Boulanger and Ziotopoulou, 2012). The DE and FD numerical models are presented in Fig. 1(a) and (b), respectively. Linear elastic 2-node beam element was used for the tunnel lining. Linear elastic solid CST element was used for

Table 1. Properties for Rock and Tunnel Lining

	Density (kg/m^3)	Elastic modulus (GPa)	Poisson's ratio
Rock	2,320	19.3	0.15
Tunnel lining	2,000	15	0.2

Table 2. Recommended Values for Normal (K_n) and Shear (K_s) Stiffness of Rock Joints

Joint type	Reference	K_n (GPa/m)	K_s (GPa/m)
Fresh to slightly weathered	Bandis *et al.* (1983)	3.6 - 22.7	0.25 - 2.36
Moderately weathered	Bandis *et al.* (1983)	4.3 - 22.5	0.47 - 1.73
Weathered	Bandis *et al.* (1983)	2.3 - 4.7	0.56 - 1.35
Soft-clay in-filling	FLAC Manual (Itasca, 2008)	0.01 - 0.1	0.01 - 0.1

intact rock block. We used the elasto-plastic model following the Mohr-Coulomb failure criterion for the joint and joint-tunnel interface. Because the deformation is expected to be concentrated in the relatively weaker joints, the assumption of an elastic behavior for intact rock blocks is justified. We used the representative values recommended by Kulhawy (1975) for clastic rock. The properties of rock and tunnel lining are presented in Table 1.

Various combinations of tunnel-joint intersection location, joint spacing, stiffness and strength, dip, interface properties, and shear strain level were modeled. The matrix of the numerical simulations is presented in Table 4. Parameters shaded in gray (case 14) represent the reference properties.

Table 3. Properties of the Rock Joints

Joint type	K_n (GPa/m)	K_s (GPa/m)	c' (MPa)	ϕ' (°)
Fresh to slightly weathered	20	2	0.2	49
Moderately weathered	5	1.3	0.1	40
Weathered	2 1	0.5 0.25	0.05 0.04	36 35
Clay-in-filled	0.1	0.025	0.03	33

To evaluate the influence of tunnel-joint intersection location

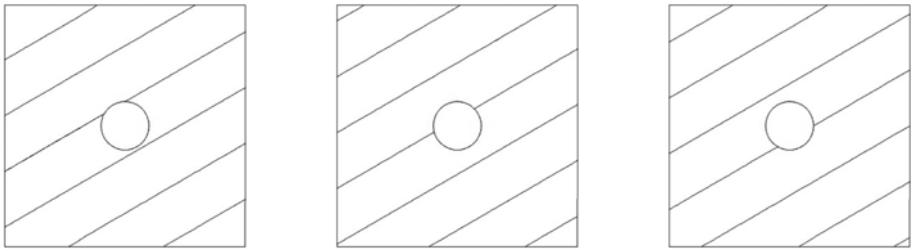

Fig. 3. Computational Model to Evaluate the Effect of Tunnel-joint Intersection Location: (a) Tunnel Crown (Case 1), (b) Tunnel Shoulder (Case 4), (c) Spring Line (Case 7)

Table 4. Matrix of Analyses

Case		Joint intersection (°)	Joint spacing (m)	Joint stiffness		Joint dip (°)	Shear strain (%)
				Normal stiffness (GPa/m)	Shear stiffness (GPa/m)		
1	Joint intersection	0	10 (1.0D)	5	1.3	30	0.01
2		15	10 (1.0D)	5	1.3	30	0.01
3		30	10 (1.0D)	5	1.3	30	0.01
4		45	10 (1.0D)	5	1.3	30	0.01
5		60	10 (1.0D)	5	1.3	30	0.01
6		75	10 (1.0D)	5	1.3	30	0.01
7		90	10 (1.0D)	5	1.3	30	0.01
8	Joint spacing	45	1 (0.1D)	5	1.3	30	0.01
9		45	1.5 (0.15D)	5	1.3	30	0.01
10		45	2 (0.2D)	5	1.3	30	0.01
11		45	2.5 (0.25D)	5	1.3	30	0.01
12		45	3 (0.3D)	5	1.3	30	0.01
13		45	3.5 (0.35D)	5	1.3	30	0.01
14		45	4 (0.4D)	5	1.3	30	0.01
15	Joint stiffness	45	4 (0.4D)	20	2	30	0.01
16		45	4 (0.4D)	2	0.5	30	0.01
17		45	4 (0.4D)	1	0.25	30	0.01
18		45	4 (0.4D)	0.1	0.025	30	0.01
19	Joint dip	45	4 (0.4D)	5	1.3	90	0.01
20		45	4 (0.4D)	5	1.3	75	0.01
21		45	4 (0.4D)	5	1.3	60	0.01
22		45	4 (0.4D)	5	1.3	45	0.01
23		45	4 (0.4D)	5	1.3	15	0.01
24		45	4 (0.4D)	5	1.3	0	0.01
25	Shear strain	45	4 (0.4D)	5	1.3	30	0.03
26		45	4 (0.4D)	5	1.3	30	0.05
27		45	4 (0.4D)	5	1.3	30	0.1

on tunnel lining response, seven sets of joints were used, which correspond to cases 1 to 7 as summarized in Table 4. 1.0 D spaced joints were used such that only a single joint intersects the tunnel. The intersection locations are successively lowered from the tunnel crown to the spring line at an interval of 15° clockwise from the center of the tunnel. The joint layouts for cases 1, 4, and 7 are shown in Fig. 3. We applied eight different values for the joint spacing, ranging from 0.1 to 1.0 D, which correspond to cases 4 and 8 to 14. The joint sets are positioned such that one joint always intersects the tunnel shoulder.

We used an elasto-plastic model following the Mohr-Coulomb failure criterion for the joint. The joint stiffness values were assigned based on the study of Bandis *et al.* (1983). The representative stiffness values reported by Bandis *et al*. (1983) for three joint types, which are fresh to slightly weathered, moderately weathered, and weathered joints, are listed in Table 2. The selected properties for normal (K_n) and shear (K_s) stiffness are summarized in Table 3. Additionally, the properties representative of the clay-infilled joint were used (Itasca Consulting Group, 2002). The representative Mohr-Coulomb strength parameters were back-calculated from the following empirical equation of Barton (1976):

$$\tau = \sigma_n \tan[JRC \log(\frac{JCS}{\sigma_n}) + \phi_r] \quad (1)$$

where σ_n is the normal stress, ϕ_r is the residual friction angle of joint, *JCS* is the joint compressive strength, and *JRC* is the joint roughness coefficient. *JCS* and *JRC* were selected from Bandis *et al.* (1983) and ϕ_r was selected from Barton (1976), respectively. The strength parameters (c', ϕ') that best fit the calculated shear strengths for σ_n from 0.2-2.0 MPa, *JCS* from 22-95, and *JRC* from 5.0-14.1 were calculated and used, as summarized in Table 3. K_n = 5 and K_s = 1.3 GPa/m were used for the tunnel-rock interface. The joint dip was varied from 90° (vertical) to 0 (horizontal), with an interval of 15. We applied four values of shear strain amplitudes, which were 0.01, 0.03, 0.05, and 0.1% (Table 4).

3. Analysis Results

The numerical analysis results are presented in this section. The DE results are compared with FD. The calculated moments and thrusts are represented as the ratio of two types of analyses, because the relative increase with respect to continuum analysis is of interest. The calculated maximum thrust and moment contours in the lining from FD are shown in Fig. 4.

We firstly evaluated the effect of the location of the tunnel-joint intersection. The calculated thrusts and moments contours in the tunnel lining for three selected cases (Case 1, 4, 7) are shown in Fig. 5. In Fig. 6, all thrusts, moments, the ratios of maximum responses from DE to FD are compared. The thrust ratios range from 1.0 to 1.7, whereas the moment ratios are significantly higher at 7.5 to 8.8. The comparisons reveal that the joint has a critical influence on the moment. A localized

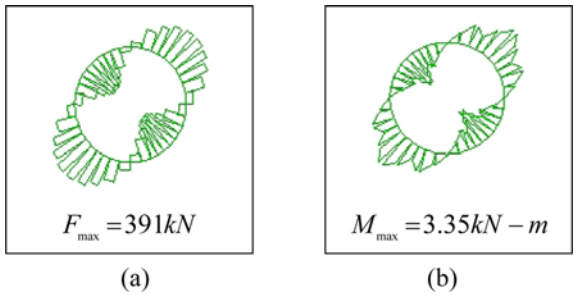

Fig. 4. Calculated Maximum Thrust and Moment from FD: (a) Thrust, (b) Moment

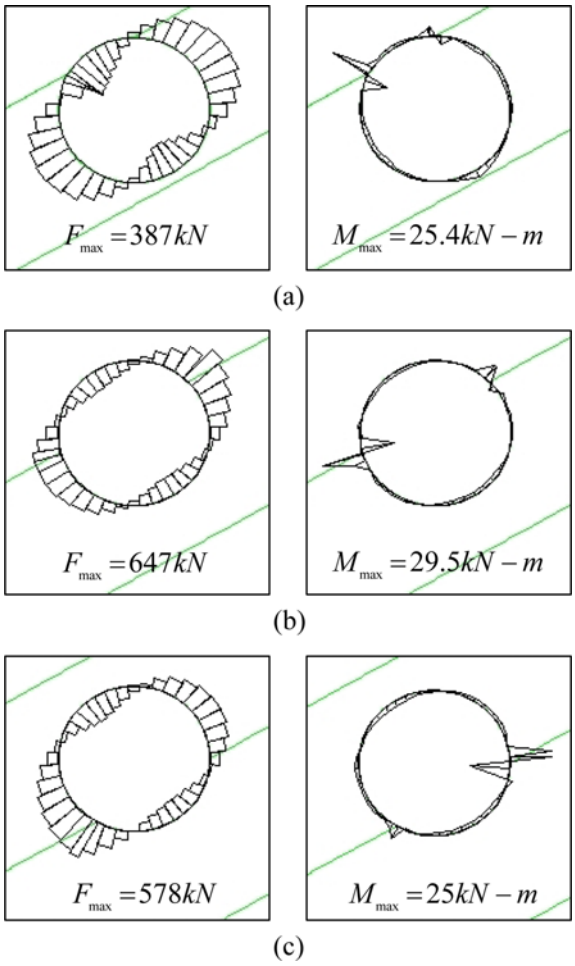

Fig. 5. Effect of Location of Joint Intersection on Calculated Thrust and Moment (Case 1, 4, 7): (a) Thrust and Moment for Case 1, (b) Thrust and Moment for Case 4, (c) Thrust and Moment for Case 7

concentration of the deformation induces corresponding increment in the moment. The influence on the thrust is much smaller in comparison. The thrust is lowest for joints intersecting the tunnel crown and 15° clockwise from the crown. The thrust increases as the location approaches the 45° intersection point. The moment is not highly influenced by the location of the intersection, resulting in similar responses for all cases.

The contours of the thrust and moments for selected joint

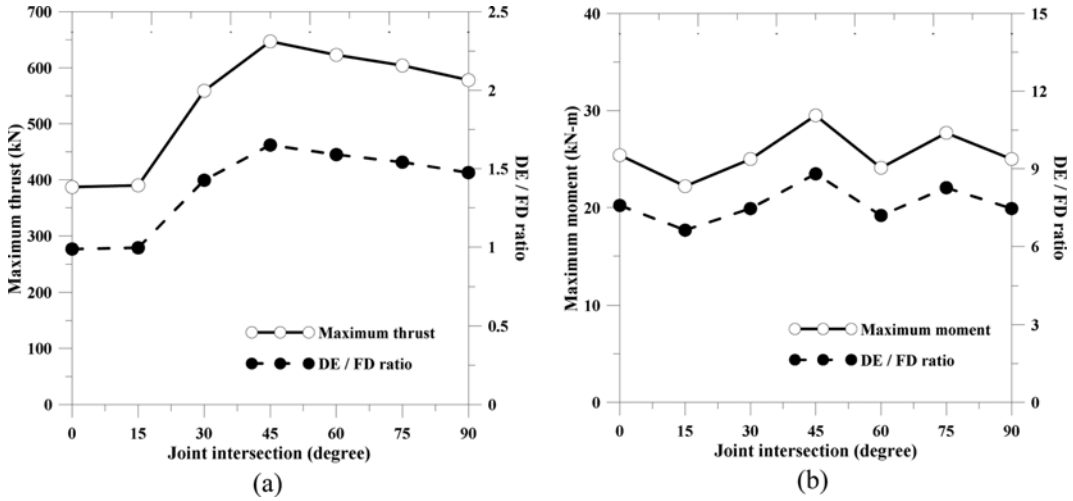

Fig. 6. Effect of Joint Intersection Location on Calculated: (a) Maximum Thrust and DE/FD Thrust Ratio, (b) Maximum Moment and DE/FD Moment Ratio (Case 1 - 7)

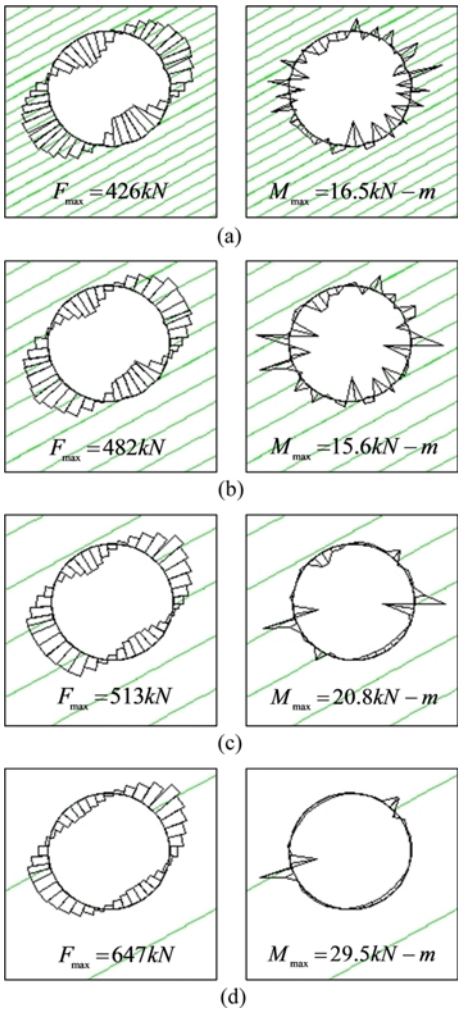

Fig. 7. Effect of Joint Spacing on Calculated Thrust and Moment (Case 4, 8, 10, 14): (a) Thrust and Moment for 0.1 D Spacing (Case 8), (b) Thrust and Moment for 0.2 D Spacing (Case 10), (c) Thrust and Moment for 0.4D Spacing (Case 14), (d) Thrust and Moment for 1.0 D Spacing (Case 4)

spacings are illustrated in Fig. 7. Fig. 8 displays all simulated thrusts, moments, and ratios. As the joint spacing decreases, the deformation becomes more uniformly distributed along the tunnel lining. As spacing increases, the response of tunnel significantly increases due to a concentration of deformation. A level of scatter is observed around the best fit linear correlation line between the calculated responses and joint spacing. It is because a change in the joint spacing is accompanied by a corresponding change in the tunnel-joint intersection location. However, a strong positive correlation with the joint spacing is clearly identified.

Figure 9 displays the influence of joint stiffness and strength on calculated response (cases 14 to 18). The effect on thrust is revealed to be very limited. However, it has a critical influence on the calculated moment. The moment ratio increases up to 20 times for weakest joint. Tunnels built in weakly jointed rock should be designed to withstand the significant localized moment. Fig. 10 shows the effect of the joint dip on the response of the tunnel lining. In Fig. 11, the ratios of peak thrust and moments from DE and FD are compared. The joints are again positioned that at least one joint intersects the tunnel at the shoulder. Pulse like concentrations of the moment and shear force are observed at tunnel-joint intersections, whereas the thrust does not result in pronounced increments. In line with previous analyses, the effect of joint dip is more prevalent on moment than on thrust. The moment is the highest for vertical and horizontal joints, and the lowest for joints with 45° dipping angle. This is because the shear stress is the largest at vertical and horizontal planes under vertically propagating shear waves.

The effect of shear strain is evaluated by comparing the results of 4, 25, 26, and 27, summarized Fig. 12. The thrusts and moments are almost linearly proportional to the shear strain amplitude. The comparisons show that if the responses are calculated for a level of the shear strain, the responses at other amplitudes can be easily estimated by through linear interpolation.

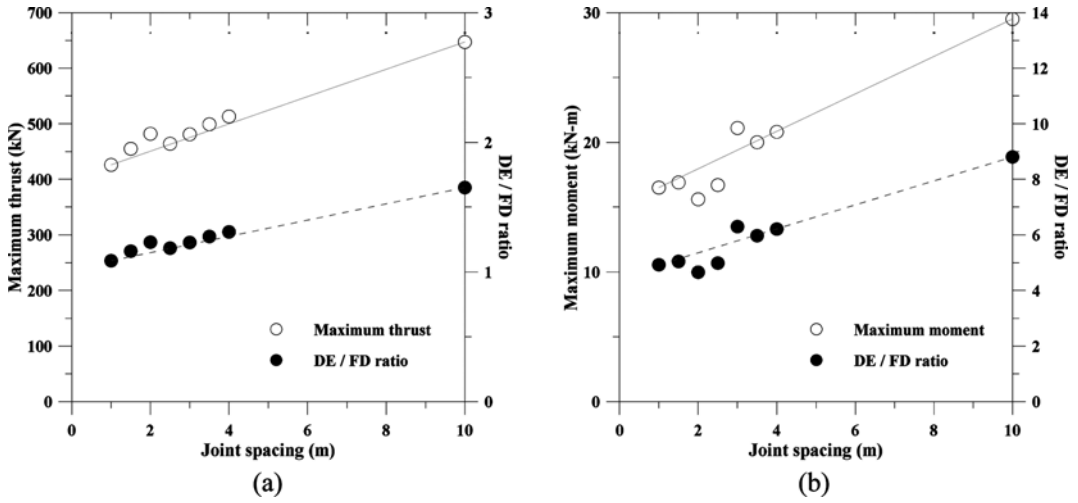

Fig. 8. Effect of Joint Spacing on Calculated: (a) Maximum Thrust and DE/FD Thrust Ratio, (b) Maximum Moment and DE/FD Moment Ratio (Cases 4, 8, 9, 10, 11, 12, 13, 14)

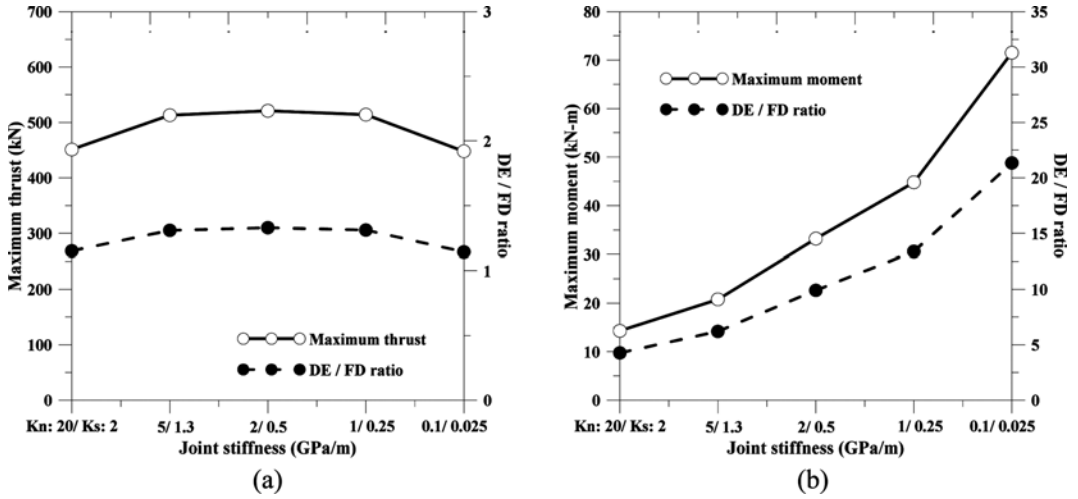

Fig. 9. Effect of Joint Stiffness and Strength on Calculated: (a) Maximum Thrust and DE/FD Thrust Ratio, (b) Maximum Moment and DE/FD Moment Ratio (Case 14, 15, 16, 17, 18)

To summarize, analyses involving various combinations of joint parameters demonstrate that the deformation in jointed rock is non-uniform and causes localized movement along the joint. This type of movement induces localized moment to develop in the tunnel lining. The pulse-like moment that develops is likely to generate small-scale cracks along the lining. Such cracks may not cause a structural collapse, but may be detrimental to the long-term serviceability of the tunnel. This may be particularly important for underground nuclear facilities built in jointed rock.

4. Conclusions

We performed a series of pseudo-static Discrete Element (DE) and finite difference analyses (FD) to evaluate the effect of joint on the seismic response of circular tunnels. Joint parameters modeled include tunnel-joint intersection location, joint spacing, joint stiffness - strength, joint dip, and shear strain level. The properties of the joint were estimated from a comprehensive literature review. The effect of various joint parameters on the calculated thrust and moment are quantified. The ratio of the thrust and moment from DE to those from FD are calculated and compared.

The joint parameters are revealed to have important impact on the calculated moment, whereas they have secondary influence on the thrust. The joint stiffness and strength have the highest influence on the moment. The tunnel response increases with joint spacing. It is largest for widely spaced joints, because of a concentration of deformation along the joint. For closely spaced joints, the response becomes similar to a continuum analysis. The tunnel-joint intersection location and joint dip are shown to have relatively lower influence on the tunnel response compared with the joint stiffness and strength. Joints intersecting the tunnel at the shoulder results in the largest thrust. The joint set dipping at 45° results in the lowest moment, because the largest shear

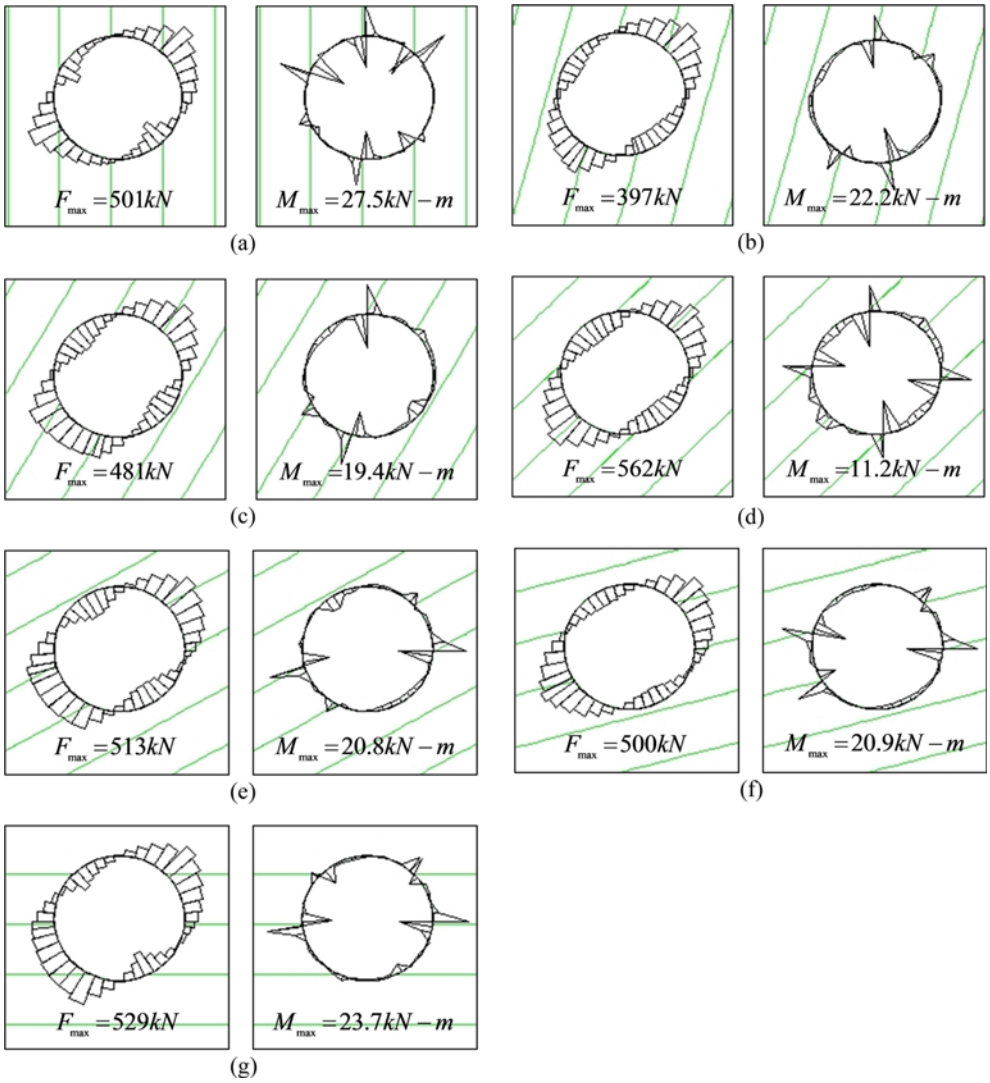

Fig. 10. Effect of Joint Dip on Calculated Thrust and Moment (Case 14, 19, 20, 21, 22, 23, 24): (a) Thrust and Moment for Case 19, (b) Thrust and Moment for Case 20, (c) Thrust and Moment for Case 21, (d) Thrust and Moment for Case 22, (e) Thrust and Moment for Case 14, (f) Thrust and Moment for Case 23, (g) Thrust and Moment for Case 24

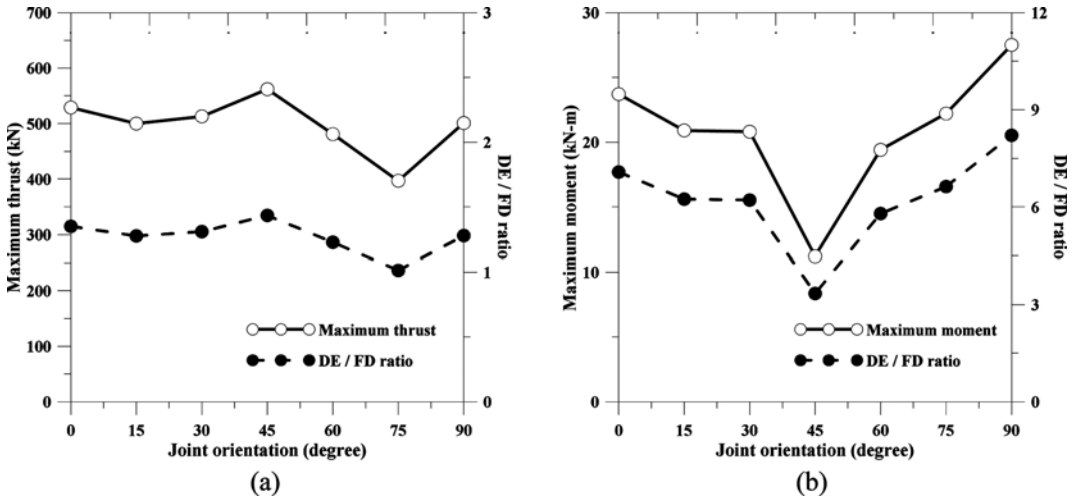

Fig. 11. Effect of Joint Dip on Calculated: (a) Maximum Thrust and DE/FD Thrust Ratio, (b) Maximum Moment and DE/FD Moment Ratio (Case 14, 19, 20, 21, 22, 23, 24)

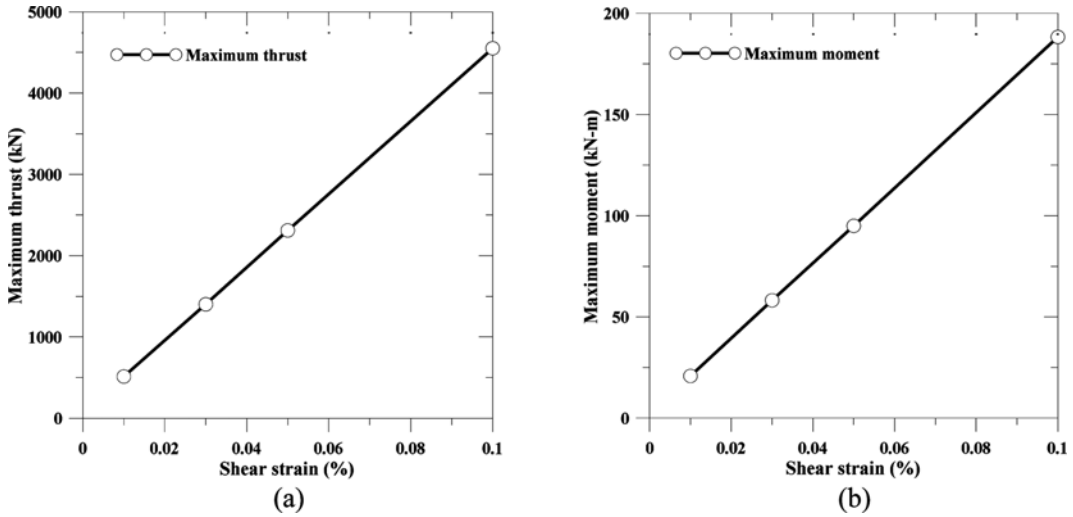

Fig. 12. Effect of Shear Strain on Calculated: (a) Maximum Thrust, (b) Maximum Moment (Case 14, 25, 26, 27)

Table 5. Calculated Maximum Thrust and Moment

Case No.	Max. thrust (kN) / Ratio[1]	Max. moment (kN-m) / Ratio[1]	Case No.	Max. thrust (kN) / Ratio[1]	Max. moment (kN-m) / Ratio[1]
1	387 / 1.0	25.4 / 7.6	15	451 / 1.2	14.3 / 4.3
2	391 / 1.0	22.2 / 6.6	16	521 / 1.3	33.2 / 9.9
3	559 / 1.4	25.0 / 7.5	17	514 / 1.3	44.8 / 13.4
4	647 / 1.7	29.5 / 8.8	18	448 / 1.2	71.5 / 21.3
5	623 / 1.6	24.1 / 7.2	19	501 / 1.3	27.5 / 8.2
6	604 / 1.5	27.7 / 8.3	20	397 / 1.0	22.2 / 6.6
7	578 / 1.5	25.0 / 7.5	21	481 / 1.2	19.4 / 5.8
8	426 / 1.1	16.5 / 4.9	22	562 / 1.4	11.2 / 3.3
9	455 / 1.2	16.9 / 5.0	23	500 / 1.3	20.9 / 6.2
10	482 / 1.2	15.6 / 4.7	24	529 / 1.4	23.7 / 7.1
11	464 / 1.2	16.7 / 5.0	25	1,402 / 3.6	58.2 / 17.4
12	481 / 1.2	21.1 / 6.3	26	2,311 / 5.9	95.0 / 28.4
13	499 / 1.3	20.0 / 6.0	27	4,551 / 11.6	188.3 / 56.2
14	513 / 1.3	20.8 / 6.2			

[1]Ratio represents the ratio of the response calculated from DE to the FD result

stresses are applied to the vertical and horizontal planes for vertically propagating shear waves.

Because a highly concentrated pulse-like moment develops due to localized joint deformation, the tunnel is highly susceptible to small-scale crack development. Prediction of this type of localized crack may be important for critical structures such as underground nuclear facilities.

Acknowledgements

This research was supported by Basic Science Research Program through the National Research Foundation of Korea (NRF) funded by the Ministry of Science, ICT and Future Planning (NRF-2015R1A2A2A01006129). The authors gratefully acknowledge this support.

References

Ahn, J. K., Park, D. H., Kim, D. K., and Kim, K. Y. (2013). "Evaluation of seismic performance of road tunnels in operation." *Journal of Korean Tunnelling and Underground Space Association*, Vol. 15, No. 2, pp.69-80.

Argyroudis, S. and Pitilakis, K. (2012), "Seismic fragility curves of shallow tunnels in alluvial deposits." *Soil Dynamics and Earthquake Engineering,* Vol. 35, pp. 1-12.

Asakura, T. and Sato, Y. (1996). "Damage to mountain tunnels in hazard area." *Soils and foundations*, pp. 301-310.

Bandis, S., Lumsden, A., and Barton, N. (1983). "Fundamentals of rock joint deformation." *Elsevier*, Vol. 20, pp. 249-268.

Barton, N. (1995). *The influence of joint properties in modelling jointed rock masses*, 8th ISRM congress: International Society for Rock Mechanics.

Barton, N. R. (1976). "The shear strength of rock and rock joints." *International Journal of Rock Mechanics and Mining Sciences*, Vol. 13, No. 9, pp. 255-279.

Bhasin, R. and Høeg, K. (1998). "Parametric study for a large cavern in jointed rock using a distinct element model (UDEC—BB)." *International Journal of Rock Mechanics and Mining Sciences*, Vol. 35, No. 1, pp.17-29.

Boulanger, R. and Ziotopoulou, K. (2012). *PM4Sand (Version 2): a sand plasticity model for earthquake engineering applications*, University of California at Davis, California.

Cilingir, U. and Gopal Madabhushi, S. (2011). "A model study on the effects of input motion on the seismic behaviour of tunnels." *Soil Dynamics and Earthquake Engineering*, Vol. 31, No. 3, pp. 452-462.

Hao, H., Wu, Y., Ma, G., and Zhou, Y. (2001). "Characteristics of surface ground motions induced by blasts in jointed rock mass." *Soil Dynamics and Earthquake Engineering*, Vol. 21, No. 2, pp. 85-98.

Hao, Y. and Azzam, R. (2005). "The plastic zones and displacements around underground openings in rock masses containing a fault." *Tunnelling and Underground Space Technology*, Vol. 20, No. 1, pp. 49-61.

Hashash, Y. M. A, Karina, K., Koutsoftas, D., and O'Riordan, N. (2010). "Seismic design considerations for underground box structures." *Earth Retention Conference*, Vol. 3, pp. 1-4.

Hashash, Y. M. A. (2002). *Seismic design of underground structures:*

Role of numerical modeling, North American Tunneling.

Hashash, Y. M. A. and Park, D. (2001). "Non-linear one-dimensional seismic ground motion propagation in the Mississippi embayment." Engineering Geology, Vol. 62, Nos. 1-3, pp. 185-206.

Hashash, Y. M. A., Marulanda, C., Ghaboussi, J., and Jung, S. (2003). "Systematic update of a deep excavation model using field performance data." *Computers and Geotechnics*, Vol. 30, pp. 477-488.

Itasca Consulting Group, I. (2002). Manual, FLAC, Itasca Consulting Group, Inc.

Itasca Consulting Group, I. (2004). UDEC Universal Distinct Element Code, User's Manual, Itasca Consulting Group, Inc.

Kulhawy, F. H. (1975). "Stress deformation properties of rock and rock discontinuities." *Engineering Geology*, Vol. 9, No. 4, pp. 327-350.

Li, J. and Ma, G. (2010). "Analysis of blast wave interaction with a rock joint." *Rock Mechanics and Rock Engineering*, Vol. 43, No. 6, pp. 777-787.

Ma, M. and Brady, B. (1999). "Analysis of the dynamic performance of an underground excavation in jointed rock under repeated seismic loading." *Geotechnical & Geological Engineering*, Vol. 17, No. 1, pp. 1-20.

MOCT (2010). *The Revision of the Road-Design Guideline (The Chapter of Tunnel)*, Ministry of Constructio and Transportation.

Penzien, J. and Wu, C. L. (1998). "Stresses in linings of bored tunnels." *International Journal of Earthquake Engineering and Structural Dynamics*, Vol. 27, pp. 283-300.

Schnabel, P. B., Lysmer, J. L., and Seed, H. B. (1972). *SHAKE: A computer program for earthquake response analysis of horizontally layered sites*, EERC-72/12, Earthquake Engineering Research Center, Berkeley, CA.

Sedarat, H., Kozak, A., Hashash, Y., Shamsabadi, A., and Krimotat, A. (2009). "Contact interface in seismic analysis of circular tunnels." *Tunnelling and Underground Space Technology*, Vol. 24, No. 4, pp. 482-490.

Seed, H. B. and Idriss, I. M. (1970). *Soil moduli and damping factors for dynamic response analyses*, University of California, Berkeley, Berkeley.

Vanmarcke, E. H., Fenton, G. A., and Heredia-Zavoni, E. (1999). *SIMQKE-II, Conditioned earthquake ground motion simulator: User's manual*, version 2.1 Princeton University, Princeton.

Vardakos, S. S., Gutierrez, M. S., and Barton, N. R. (2007). "Back-analysis of Shimizu Tunnel No. 3 by distinct element modeling." *Tunnelling and Underground Space Technology*, Vol. 22, No. 4, pp. 401-413.

Wang, J. (1993). "Seismic design of tunnels: A state-of-the-art approach, Parsons Brinckerhoff Quade & Douglas." Inc., New York, NY, Monograph 7.